Electronic Supplementary Material (ESI) for Analyst.
This journal is © The Royal Society of Chemistry 2015

Two fluorescent Schiff base sensors for Zn^{2+}: the Zn^{2+}/Cu^{2+} ion interference

Arturo Jiménez-Sánchez,[a] Benjamín Ortíz,[b] Vianney Ortiz Navarrete,[b] Norberto Farfán,[c] and Rosa Santillan*[a]

[a] Departamento de Química, Centro de Investigación y de Estudios Avanzados del IPN, Apdo. Postal 14-740, 07000, México, D.F., México.

[b] Departamento de Biomedicina Molecular, Centro de Investigación y de Estudios Avanzados del IPN, Apdo. Postal 14-740, 07000, México, D.F., México.

[c] Facultad de Química, Departamento de Química Orgánica, Universidad Nacional Autónoma de México, Ciudad Universitaria 04510, México D.F., México.

Correspondence should be addressed to e-mail: rsantill@cinvestav.mx

Supplementary Information

CONTENTS PAGE

Experimental

All reagents and solvents are commercially available and used as received. The solvents were HPLC grade. The ^{1}H and ^{13}C NMR spectra were recorded on a JEOL ECA+500, using CD_3OD and $CDCl_3$ as solvent. Chemical shifts were reported in parts per million (ppm) relative to internal TMS. Mass spectra were recorded with an Agilent Technologies MS TOF using the ESI(+) technique. UV-vis absorption spectra were recorded in a Perkin Elmer UV/VIS Spectrophotometer Lambda 12 and fluorescence spectra in a Varian Cary Eclipse Fluorescence Spectrometer. All fluorescence quantum yield measurements were obtained by using the experimental procedure reported in reference 19 from main text, reference 1 from ESI.

Synthesis and characterization of L1 and L2

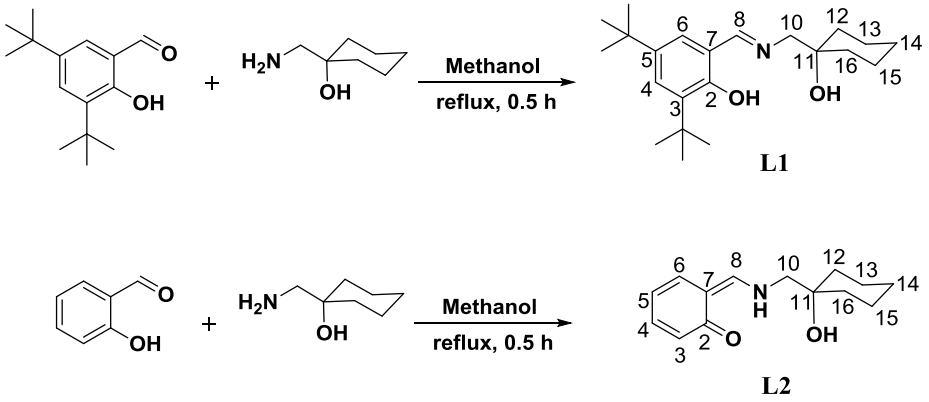

Scheme S1. Synthetic methodology for **L1** and **L2**.

2,4-di-tert-butyl-6-[(1-hydroxycyclohexylmethylimino)methyl]phenol (**L1**). The title compound was synthesize by subtle modifications of a previously reported methodology [2] from 3,5-di-*tert*-butyl salicylaldehyde 0.50 g (2.13 mmol) and 1-aminomethyl-1-cyclohexanol hydrochloride 0.35 g (2.13 mmol) under reflux of methanol for 30 min, using a Dean-Stark trap to give a yellow powder in >90% yield of **L1**. m.p.: 98-100 °C. IR (KBr) ν_{max}: 3438 (OH), 2958, 2935, 2866, 1628 (C=N), 1596, 1474, 1441, 974, 887, 852, 715 cm^{-1}. ^{1}H NMR ($CDCl_3$, 400 MHz) δ: 13.59 (1H, br, OH), 8.37 (1H, s, H-8), 7.40 (1H, d, J = 2.3 Hz, H-4), 7.11 (1H, d, J = 2.3 Hz, H-6), 3.58 (2H, s, CH2-10), 1.72-.1.47 [10H, m, $(-CH_2-)_5$], 1.45 [9H, s, $-C(CH_3)_3$], 1.31 [9H, s, $-C(CH_3)_3$]. ^{13}C NMR ($CDCl_3$, 100 MHz) δ: 168.1 (C-8), 158.2 (C-2), 140.3 (C-5), 136.8 (C-3), 127.2 (C-4), 126.2 (C-6), 117.9 (C-7), 71.6 (C-11), 70.4 (C-10), 35.9 (C-12 and C-16), 35.1 ($-C(CH_3)_3$), 34.2 ($-C(CH_3)_3$), 31.6 ($-C(CH_3)_3$), 29.5 ($-C(CH_3)_3$), 26.0 (C-14), 22.0 (C-13 and C-15). Anal. Calcd. for $C_{22}H_{35}N_1O_2$: C 76.48, H 10.21, N 4.05; found: C 76.42, H 10.18, N 4.18. HR-APCI-MS: *m/z* for $C_{22}H_{35}NO_2$ $[M + H]^+$ calc.: 346.2741, found: 346.2745.

2-[{(1-hydroxylcyclohexyl)methylimino}methyl]phenol (**L2**). The title compound was prepared from salicylaldehyde 0.20 g (1.64 mmol) and 1-aminomethyl-1-cyclohexanol hydrochloride 0.27 g (1.64 mmol) under reflux for 30 min, to give 0.36 g (1.55 mmol, 95% yield) of **L2**. m.p.: 156-158 °C. IR (KBr) ν_{max}: 3221 (NH), 3050, 2925, 2850, 1644 (C=O), 1611 (C=N), 1524,

1288, 1146, 912, 742 cm^{-1}. ^{1}H NMR ($CDCl_3$, 400 MHz) δ: 13.41 (1H, br, OH), 8.35 (1H, s, H-8), 7.32-7.26 (2H, m, H-4 and H-6), 6.96-6.90 (1H, m, H-3), 6.89-6.86 (1H, m, H-5), 3.58 (2H, s, CH_2-10), 2.16 (1H, s, br, OH), 1.72-1.53 (8H, m, CH_2-12, CH_2-13, CH_2-15 and CH_2-16), 1.33-1.28 (2H, m, CH_2-14). ^{13}C NMR ($CDCl_3$, 100 MHz) δ: 166.9 (C-8), 161.3 (C-2), 132.5 (C-4), 131.5 (C-6), 118.9 (C-7), 118.7 (C-5), 117.2 (C-3), 71.5 (C-11), 70.2 (C-10), 35.8 (C-12 and C-16), 25.8 (C-14), 21.9 (C-13 and C-15). Anal. Calcd. for $C_{14}H_{19}N_1O_2$: C 72.07, H 8.21, N 6.00; found: C 72.16, H 8.19, N 6.12. HR-APCI-MS: m/z for $C_{14}H_{19}NO_2$ $[M + H]^+$ calc.: 234.1489, found: 234.1491.

Figure S1. UV-Vis and Fluorescence spectra for the titration of (a) **L1** and (b) **L2** with Co^{2+}, K^+, Li^+, Na^+, Pb^{2+}, Cd^{2+}, Ni^{2+}, Hg^{2+}, Cu^{2+} and Ca^{2+}. The Stock solutions of metal acetates (1 x 10^{-4} mol L^{-1}) and **L1** / **L2** (1 x 10^{-5} mol L^{-1}) were prepared in water and water : methanol (95 : 5, v/v), respectively.

(a)

$(CH_3COO)_2Co \cdot 4H_2O$:

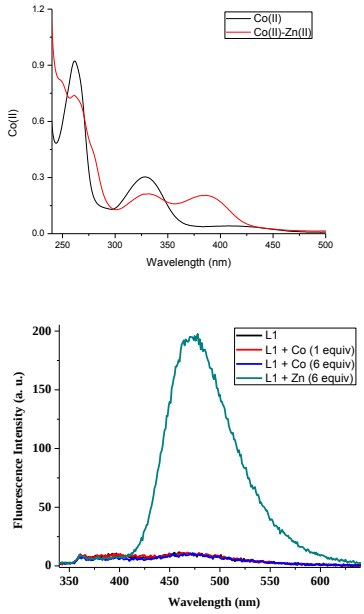

$(CH_3COO)K$:

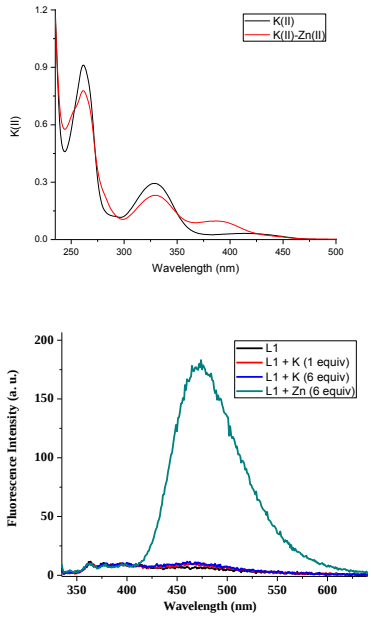

$(CH_3COO)Li$:

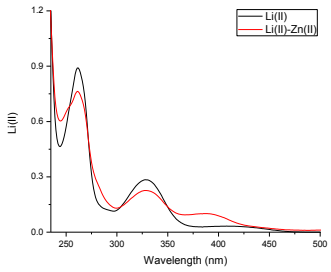

$(CH_3COO)Na$:

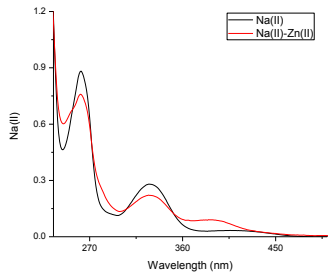

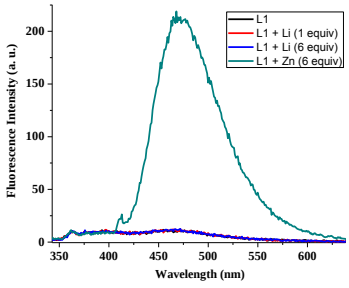

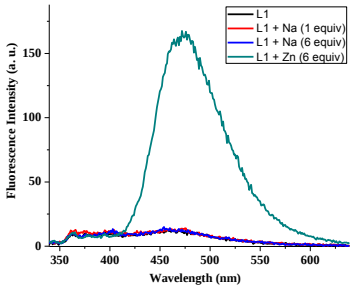

$(CH_3COO)_2Pb \cdot 3H_2O$:

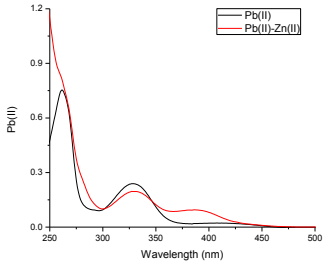

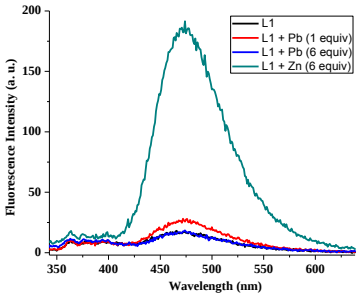

$(CH_3COO)_2Cd \cdot 2H_2O$:

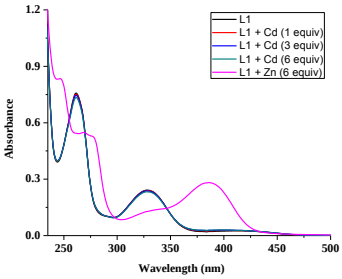

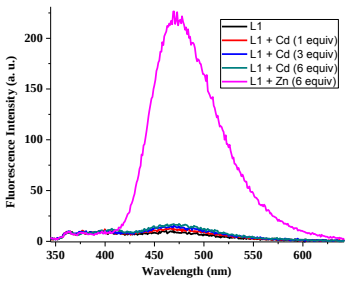

$(Cl)_3Fe$:

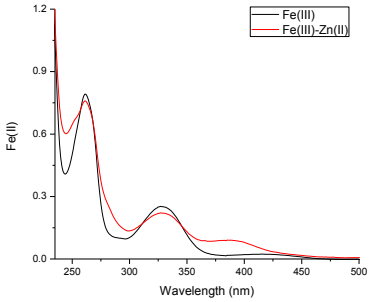

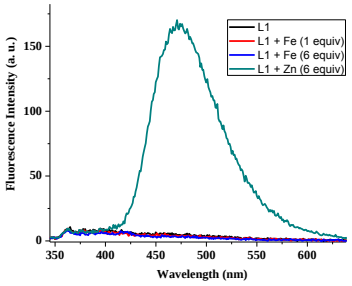

$(CH_3COO)_2Ni \cdot 4H_2O$:

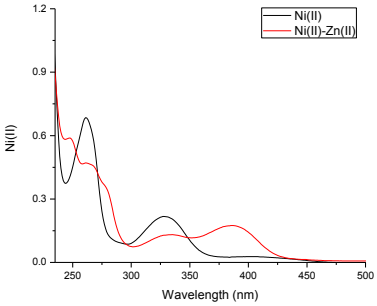

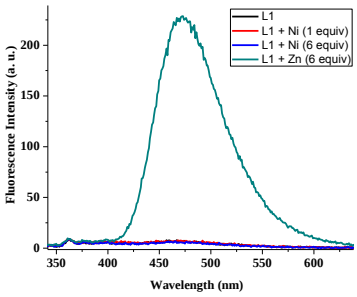

$(CH_3COO)_2Ca$:

$(CH_3COO)_2Hg$:

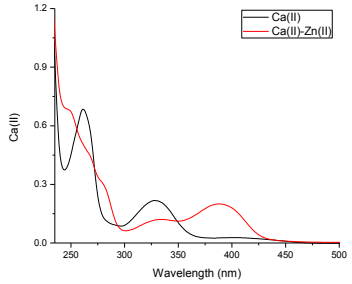

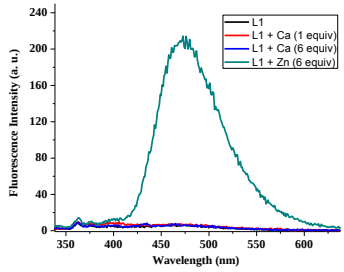

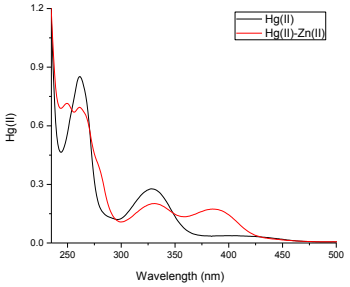

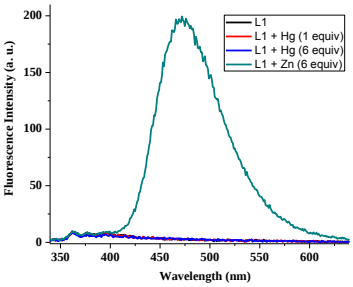

$(CH_3COO)_2Cu$:

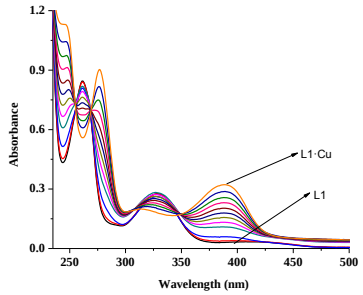

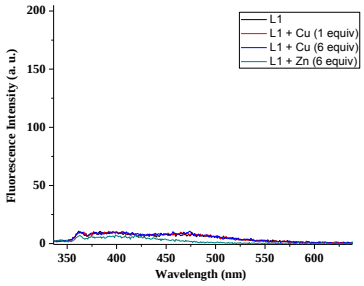

(b)

$(CH_3COO)_2Co \cdot 4H_2O$:

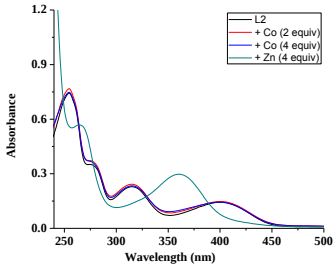

$(CH_3COO)K$:

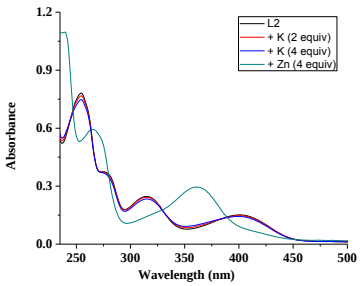

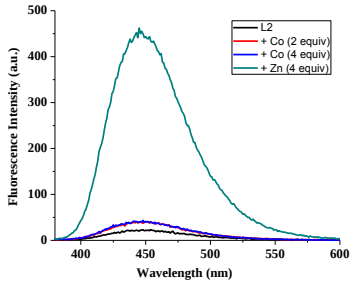

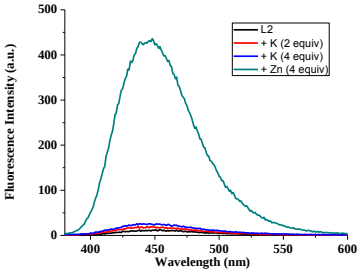

$(CH_3COO)Li$:

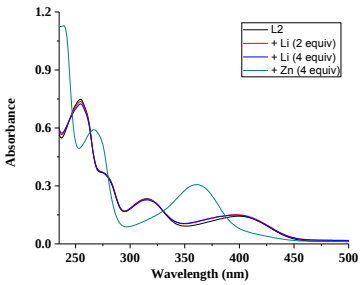

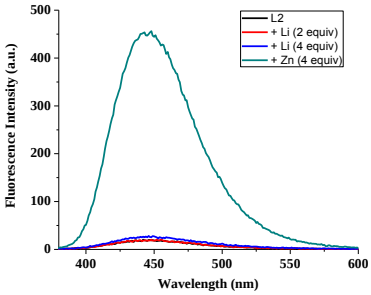

$(CH_3COO)Na$:

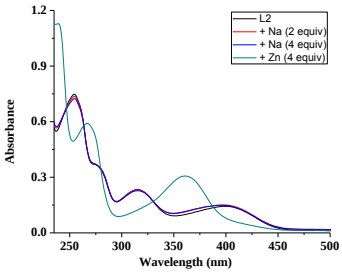

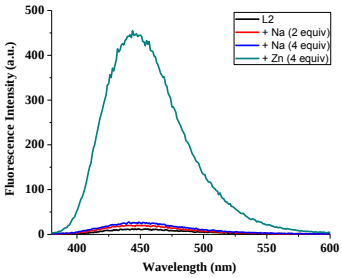

$(CH_3COO)_2Pb \cdot 3H_2O$:

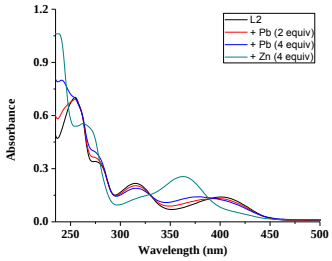

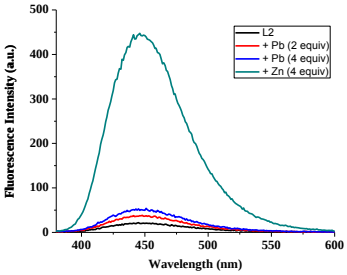

$(CH_3COO)_2Cd \cdot 2H_2O$:

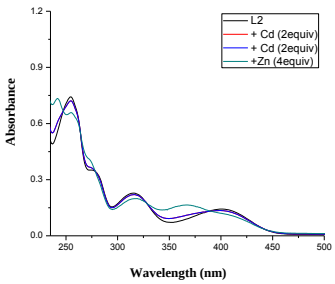

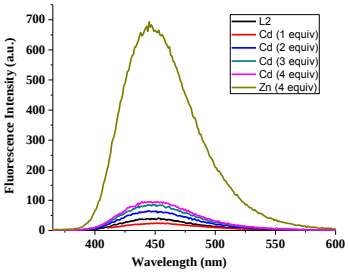

$(Cl)_3Fe$:

$(CH_3COO)_2Ni \cdot 4H_2O$:

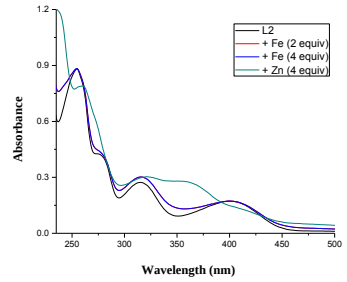

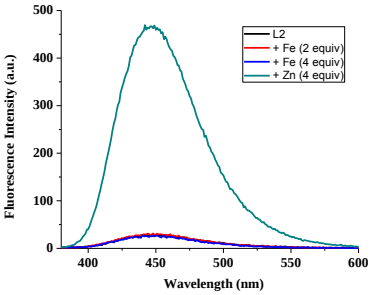

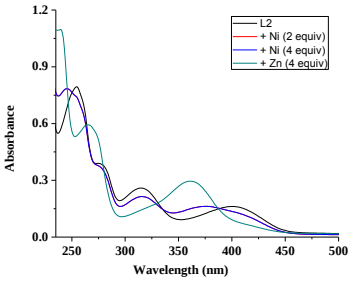

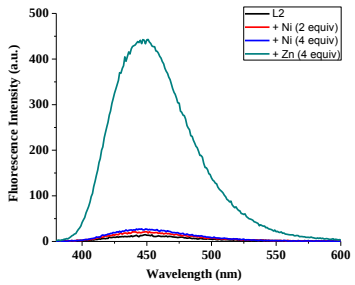

$(CH_3COO)_2Ca$:

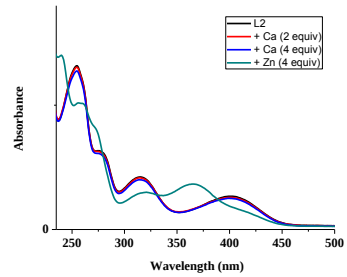

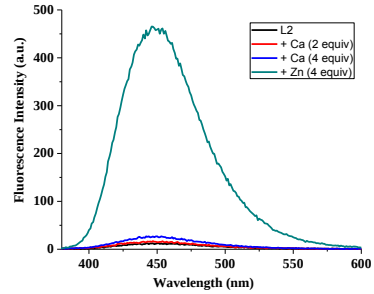

$(CH_3COO)_2Hg$:

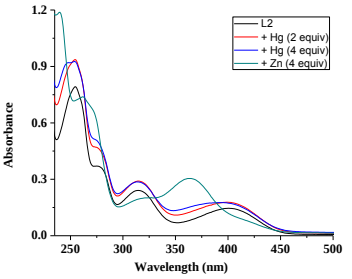

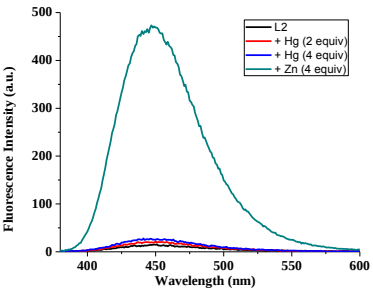

$(CH_3COO)_2Cu$:

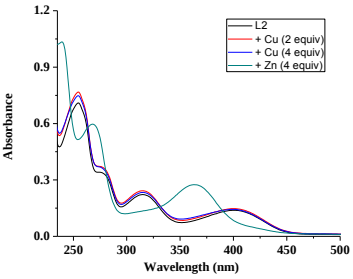

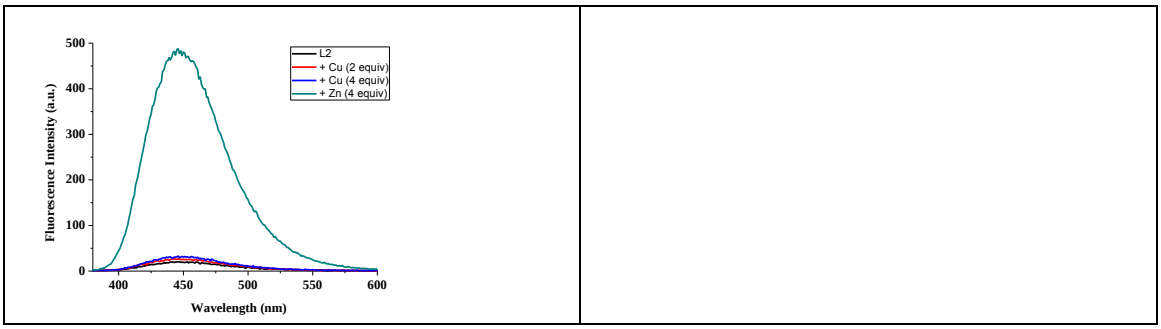

L1 **L2**

Figure S2. X-ray structures for **L1** and **L2** (CCDC reference number 712147 and 712149, respectively. O. Domínguez, B. Rodríguez-Molina, M. Rodríguez, A. Ariza, N. Farfán and R. Santillan, *New J. Chem.*, 2011, **35**, 156.).

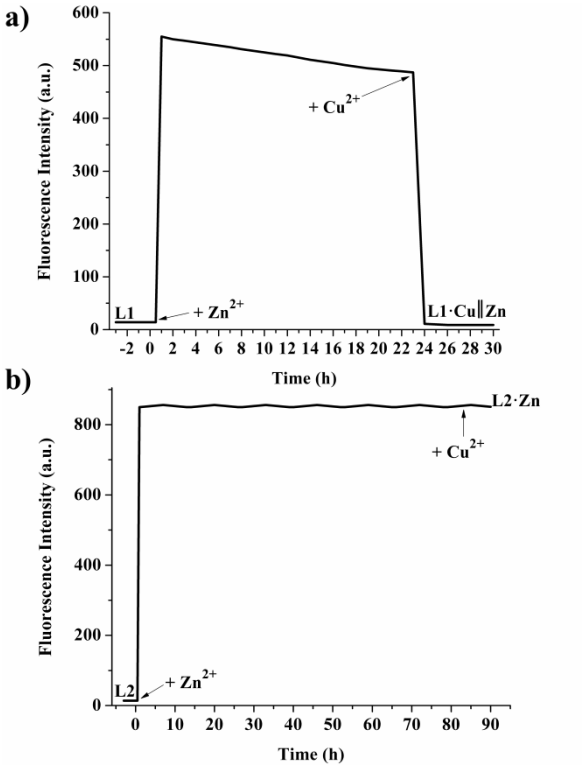

Figure S3. Fluorescence kinetics for: a) **L1** (2 mM) upon addition of Zn^{2+} (t = 120 s) to form **L1•Zn** and Cu^{2+} (t = 23 h) to form **L1•Cu**; and b) **L2** (2 mM) upon addition of Zn^{2+} (t = 120 s) to form **L2•Zn** and Cu^{2+} (t = 83 h) remaining the **L2•Zn** complex.

Figure S4. HyperQuad log K_a refinement for L-Zn complexes and Hill plots for association constants (log K_a) of Zn^{2+}/Cu^{2+} based on (log(Y/1 - Y)) n log [M^{2+}] + log K).

(a)

L2-Zn in 1:1 relation

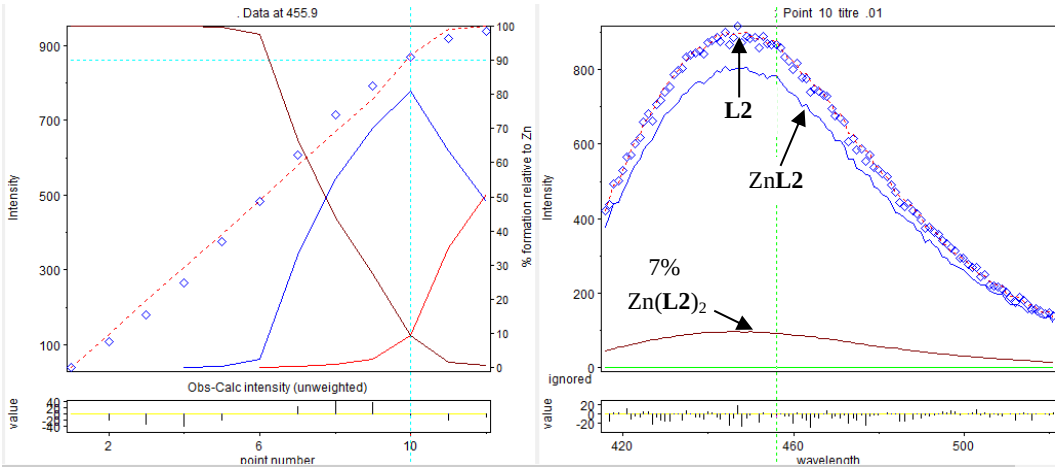

L2-Zn in 1:2 relation

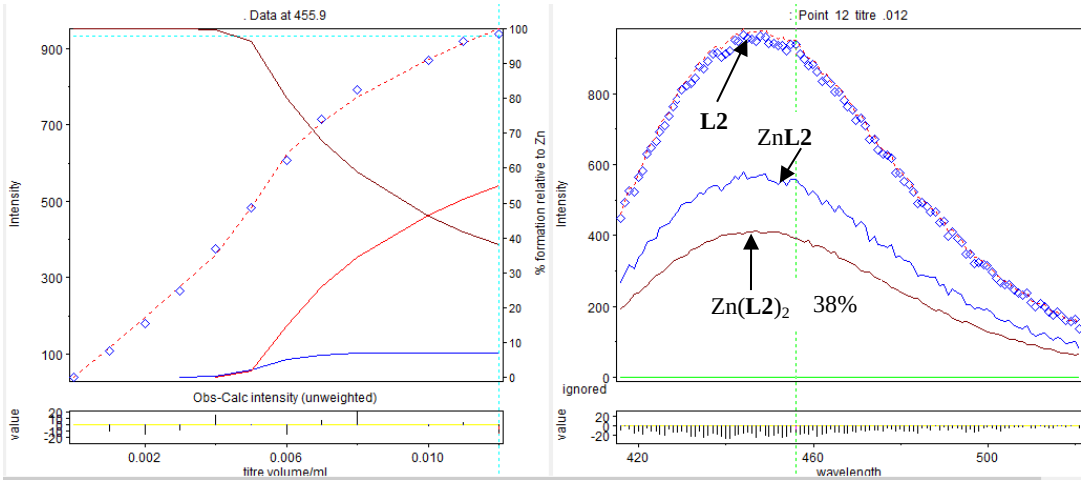


```
HypSpec. Refinement concluded at 02/06/2015 04:43:21 p. m.
Data from C:\Users\ARTURO JIMÉNEZ\Desktop\tBSZn.HQD (modified)
Project title:
 25 (maximum) Iterations performed

                    standard
Log beta    value   deviation
ZnL         8.4465  0.0789
ZnL2        10.8138 0.0972

Correlation coefficients
  2      1.0
        1
Parameter numbers
 1 ZnL
 2 ZnL2
```

Hill Plot for L2-Zn:

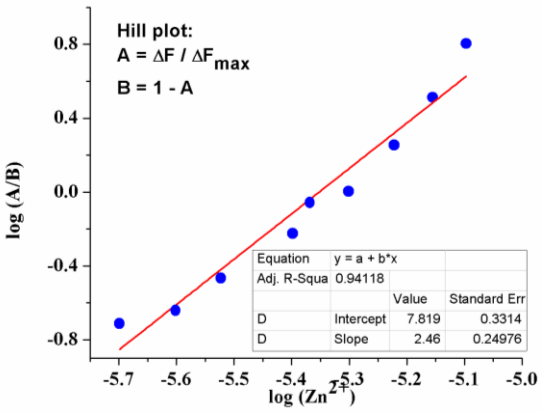

(b)

L1-Zn

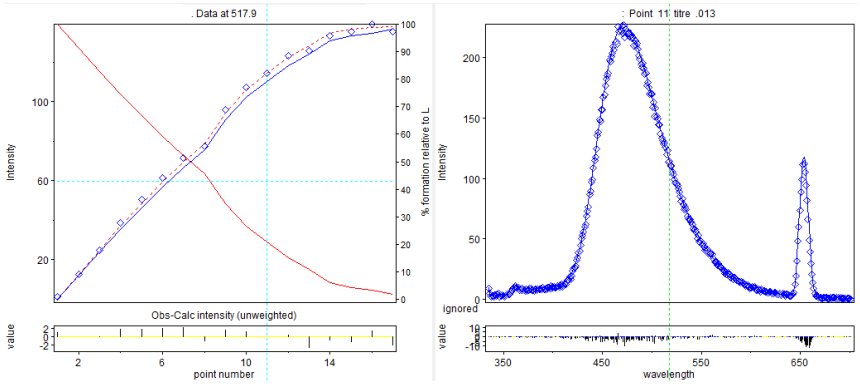


```
HypSpec. Refinement concluded at 24/10/2014 04:25:36 p. m.
Project title: L1-Zn
Converged in 11 iterations with sigma = 4.0003

                    standard
Log beta   value    deviation
LZn        5.2771   0.0048
```

Hill plot

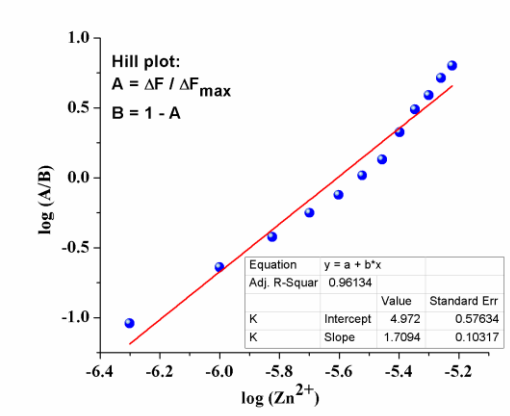

L1-Cu

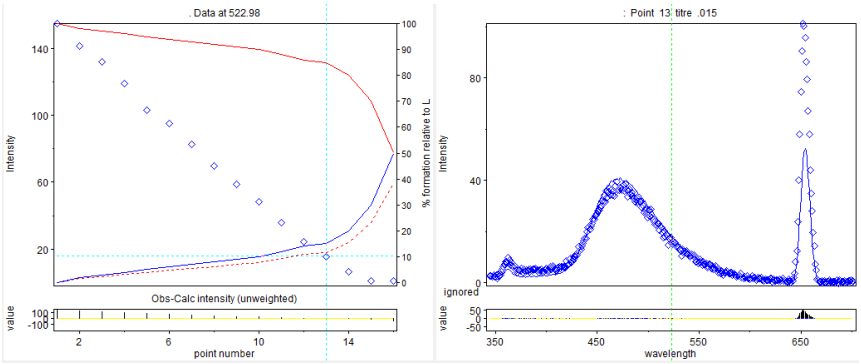


```
HypSpec. Refinement concluded at 24/10/2014 06:50:39 p. m.
Project title:
Converged in 8 iterations with sigma = 5.698

                        standard
Log beta    value       deviation
LCu         8.5416      0.062
```

Figure S5. UV-Vis spectra for **L1** and **L1•Zn** solvent polarity effect

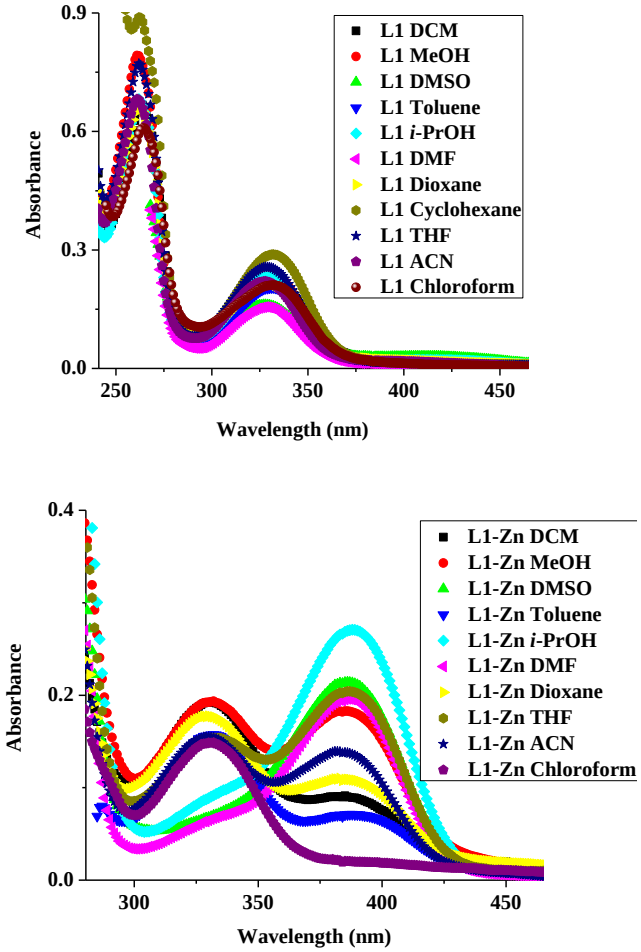

Figure S6. ^{1}H NMR spectra for **L1** and **L2** upon addition of Zn^{2+} and Cu^{2+} in DMSO-d_6:

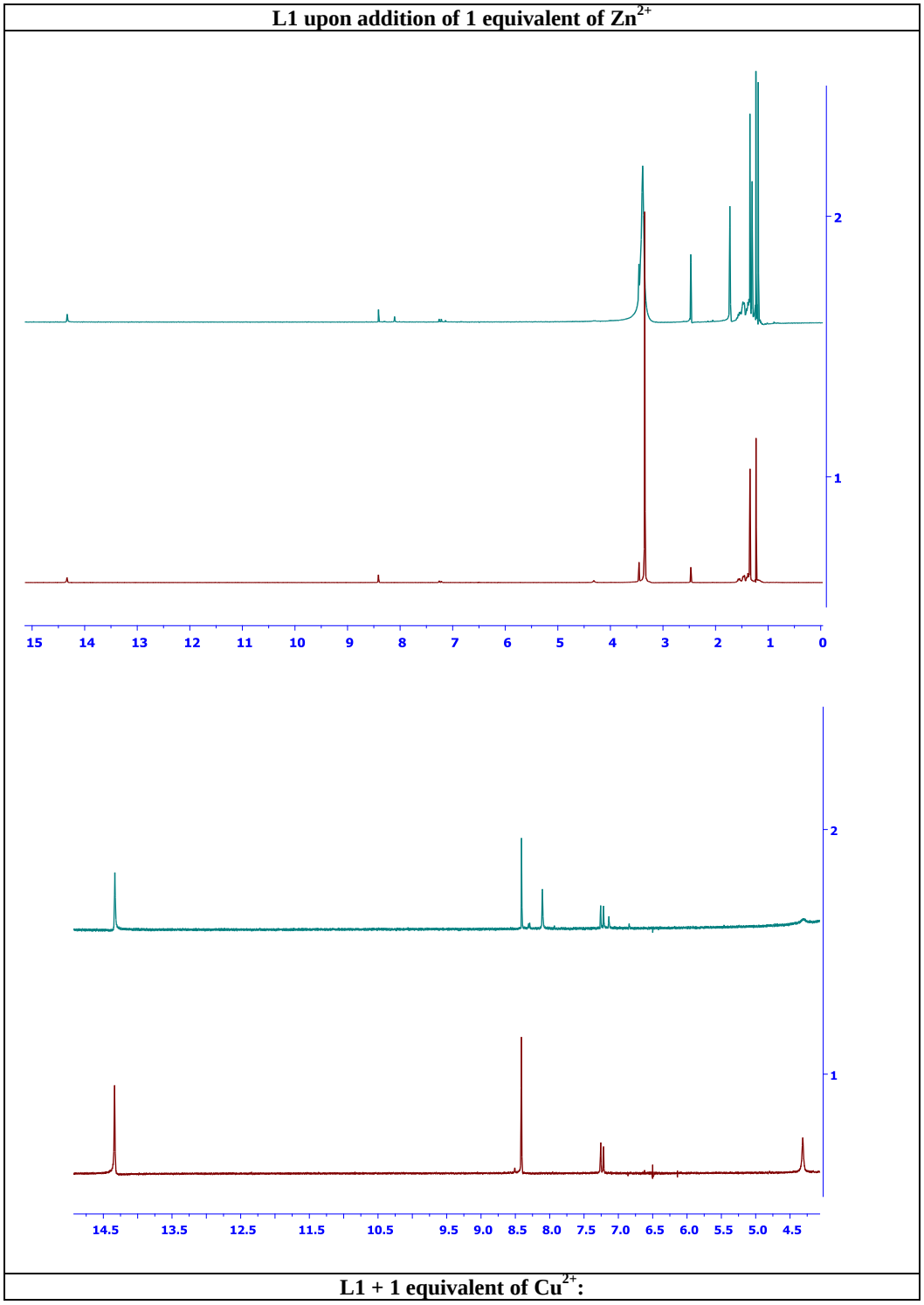

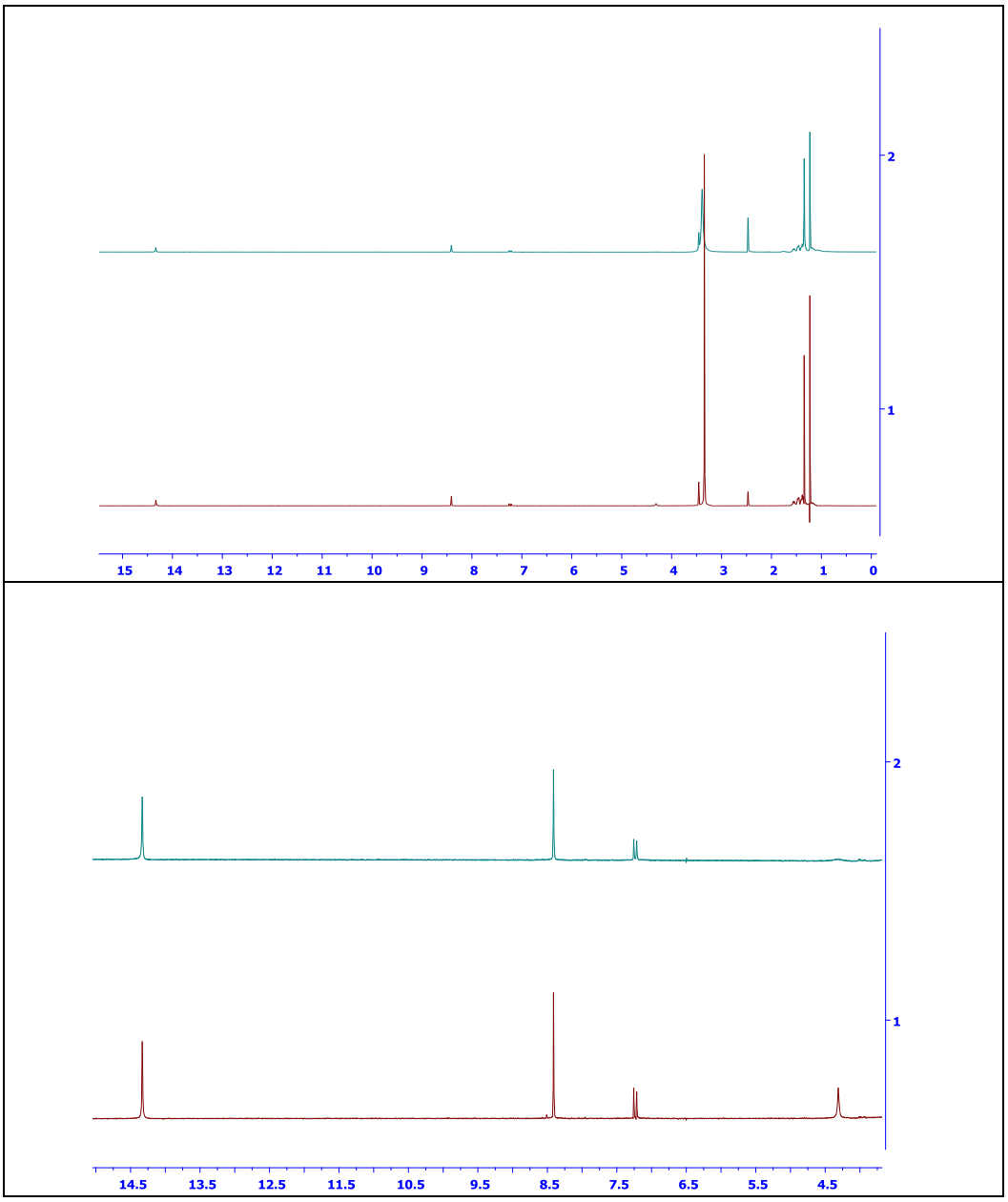
2
1
15 14 13 12 11 10 9 8 7 6 5 4 3 2 1 0
2
1
14.5 13.5 12.5 11.5 10.5 9.5 8.5 7.5 6.5 5.5 4.5

L2 upon addition of 1 equivalent of Zn^{2+}:

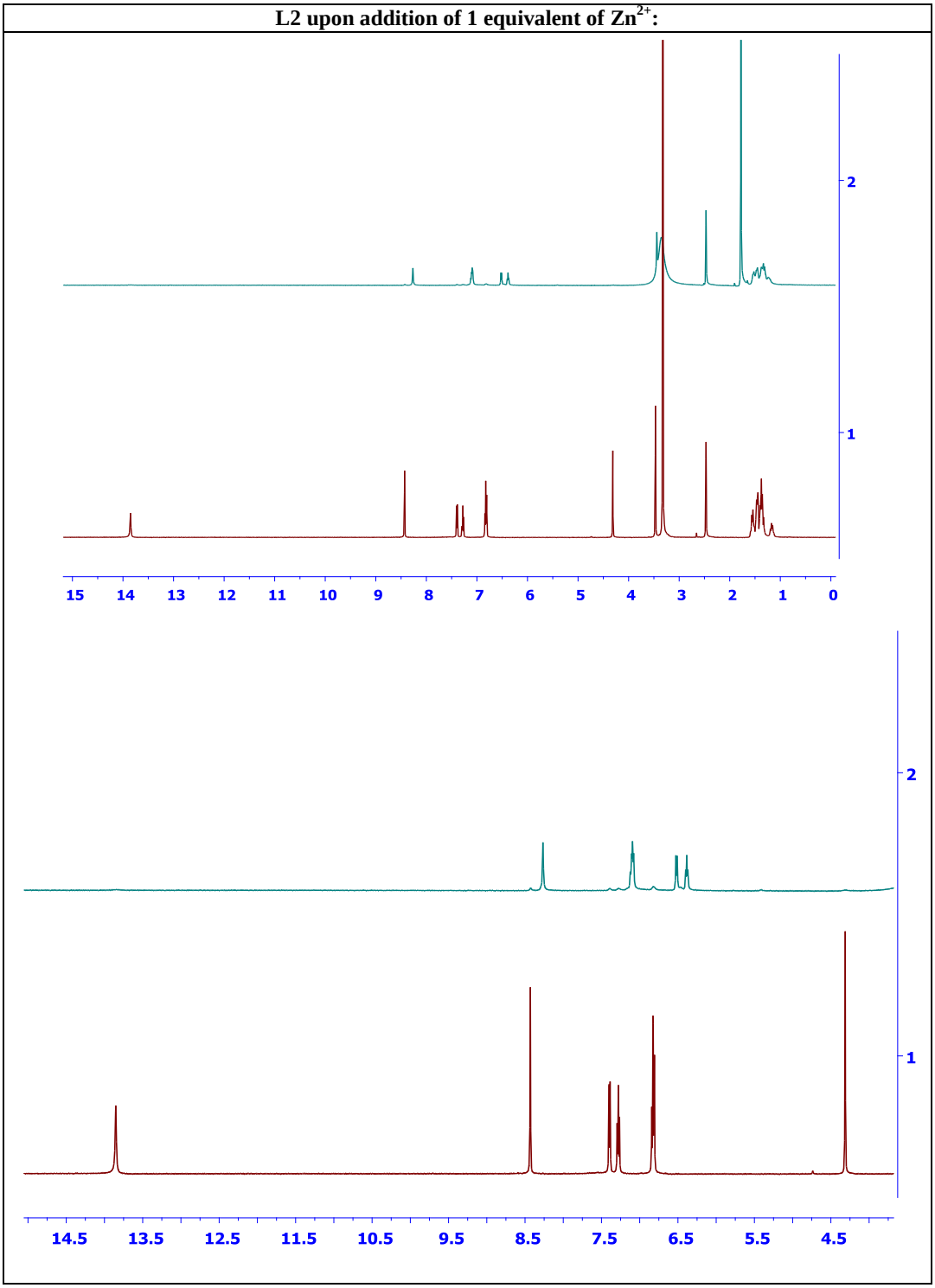

L1 upon addition of 1 equivalent of Fe^{2+}:

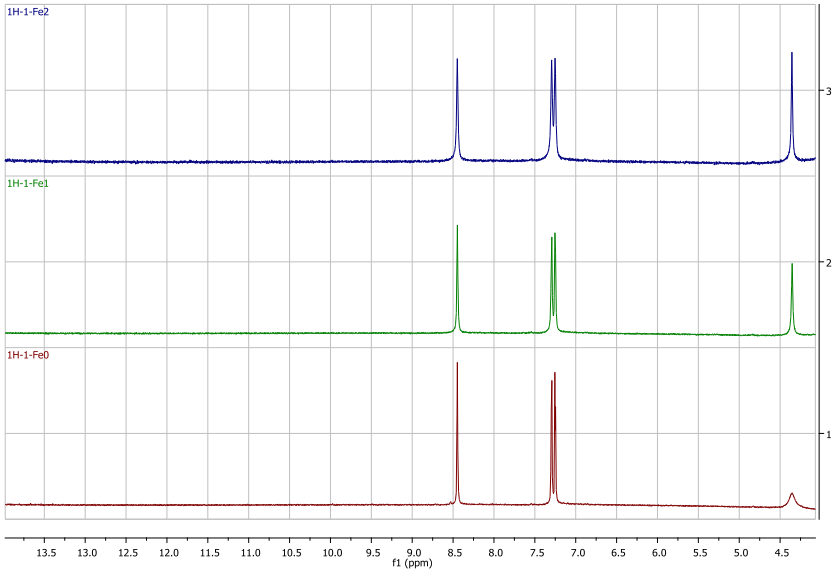

L2 upon addition of 1 equivalent of Fe^{2+}:

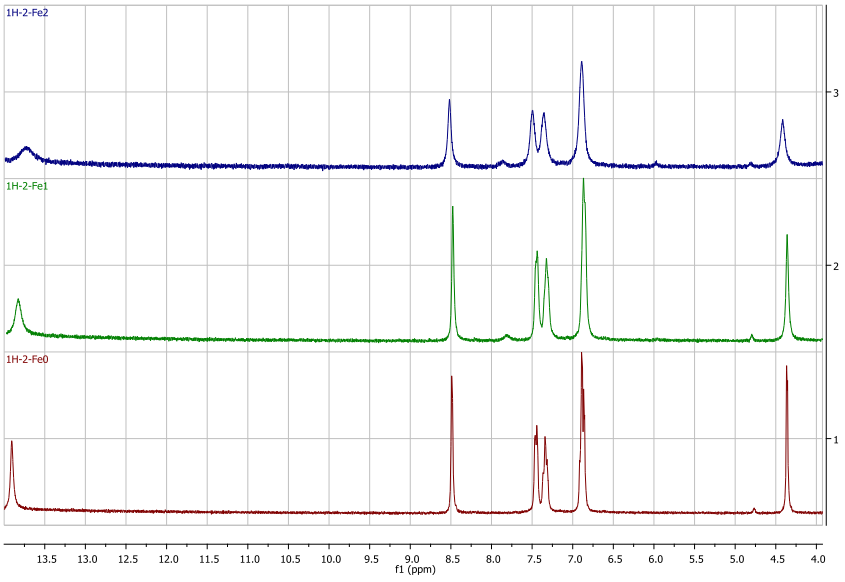

Figure S7. UV-Vis spectra for sodium tartrate anion interaction with **L2•Zn**

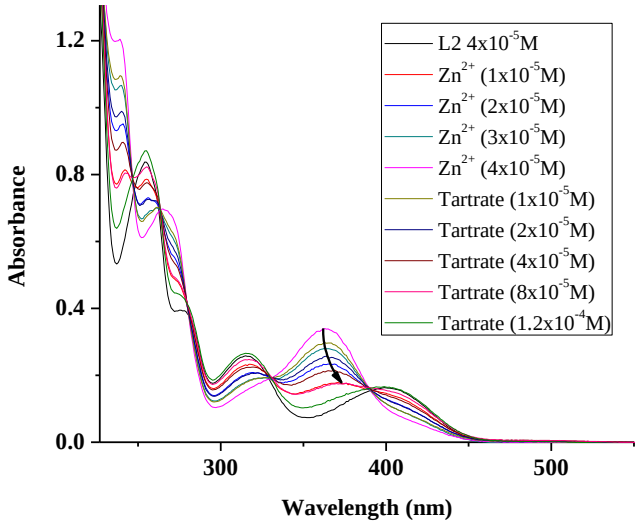

Figure S8. UV-Vis spectra for Adenosine 5′-triphosphate disodium salt hydrate interaction with **L2•Zn**

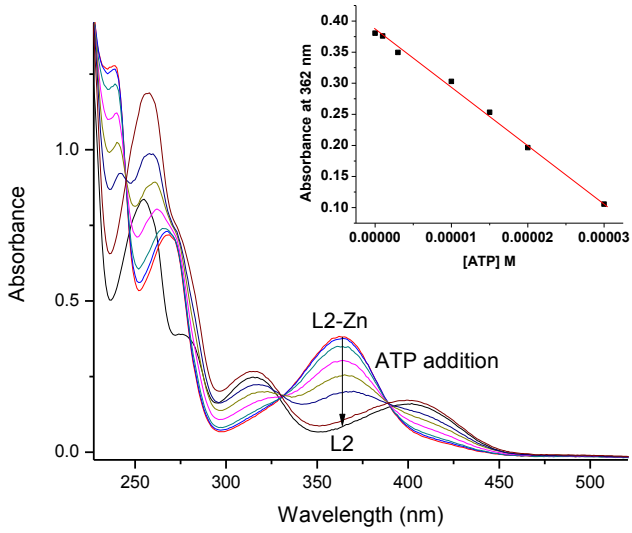

Figure S9. Absorption spectra showing the colorimetric response process for **L1** and **L2** in the presence of Fe^{2+} ions in water : methanol solution (95 : 5, v/v, 10 mM HEPES) (a). Color changes upon addition of 2 equiv. of different ions to: (b) **L1** and (c) **L2**, in the visible (above) and under 365 nm UV-light (below).

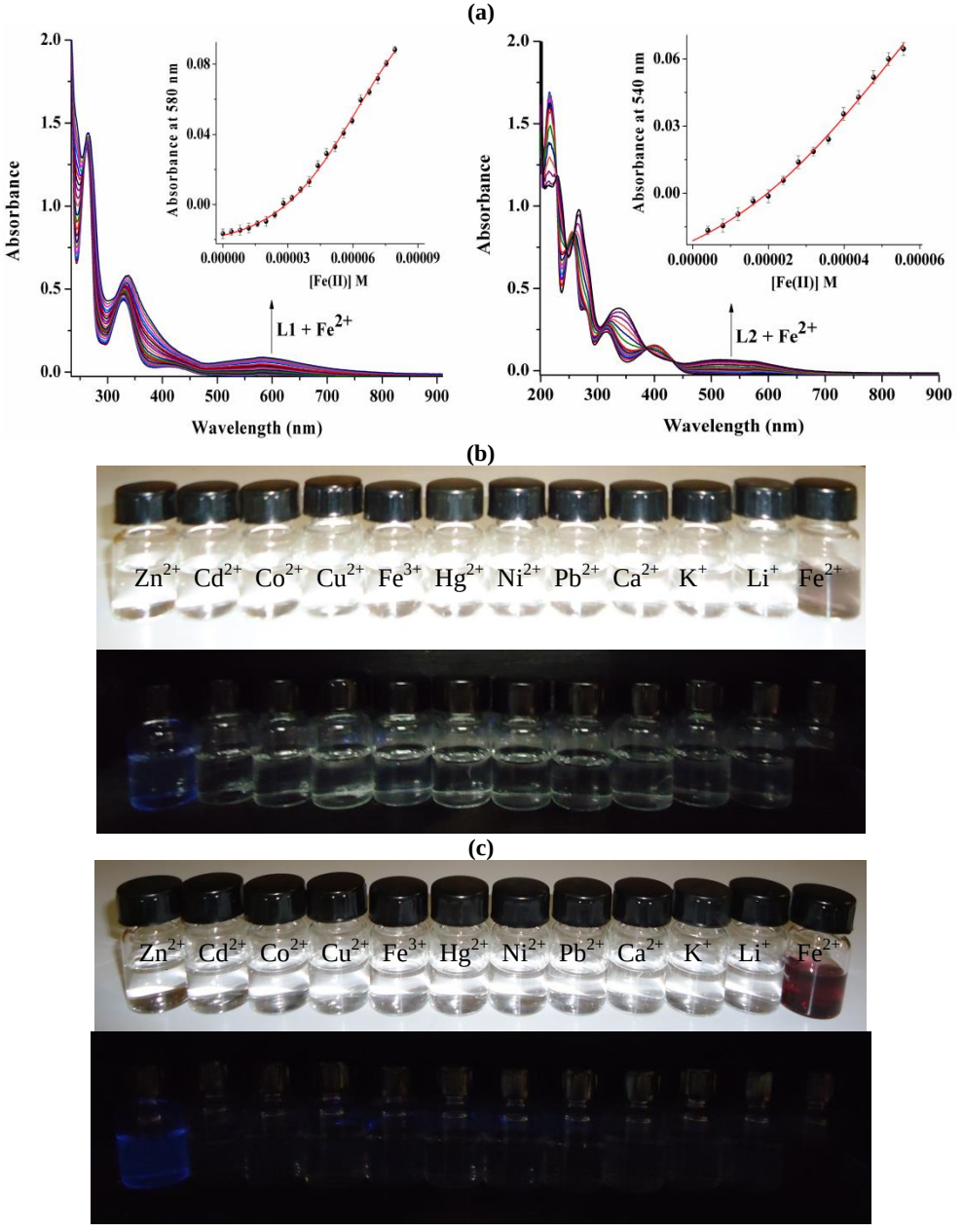

Figure S10. Spectrophotometric titration for the pH profile of (a) **L1** and (b) **L2** in acid (left) and basic (right) media.

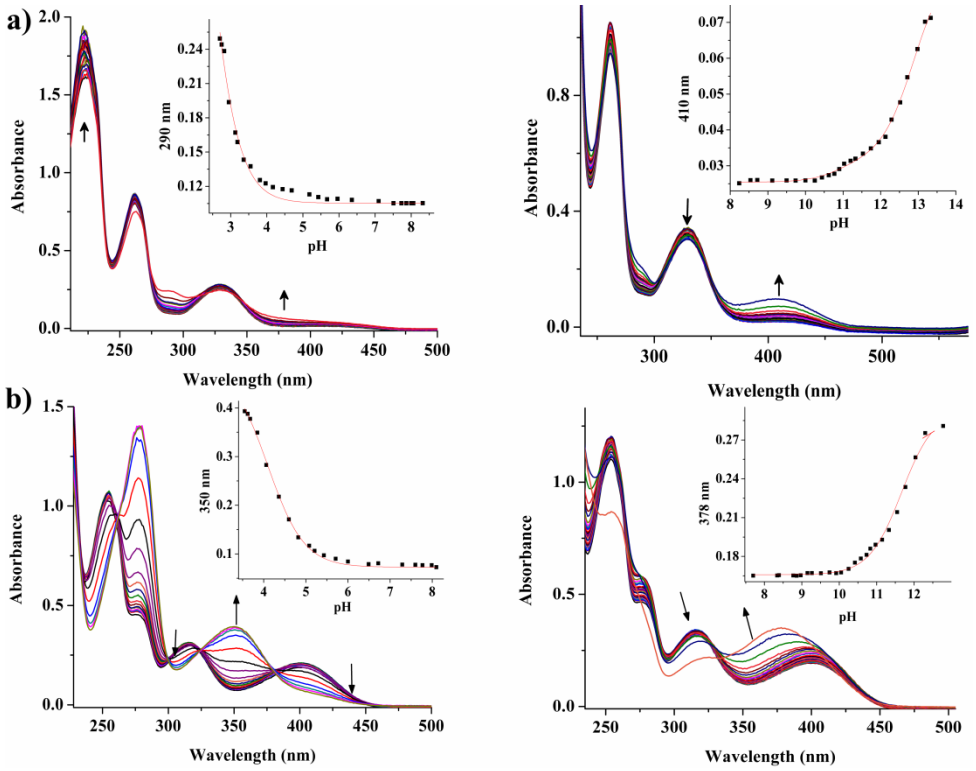

Figure S11. Fluorescence spectra of **L1** in a sample containing both, Zn^{2+} and Cu^{2+} metal ions. Gray line, no fluorescence response was observed upon addition of **L1** to the Cu^{2+} saturated solution; and blue line, the observed fluorescence response upon addition of S^{2-} anions, indicating the presence of Zn^{2+} and Cu^{2+} in the same test sample. Excitation wavelength at λ_{ex} = 365 nm.

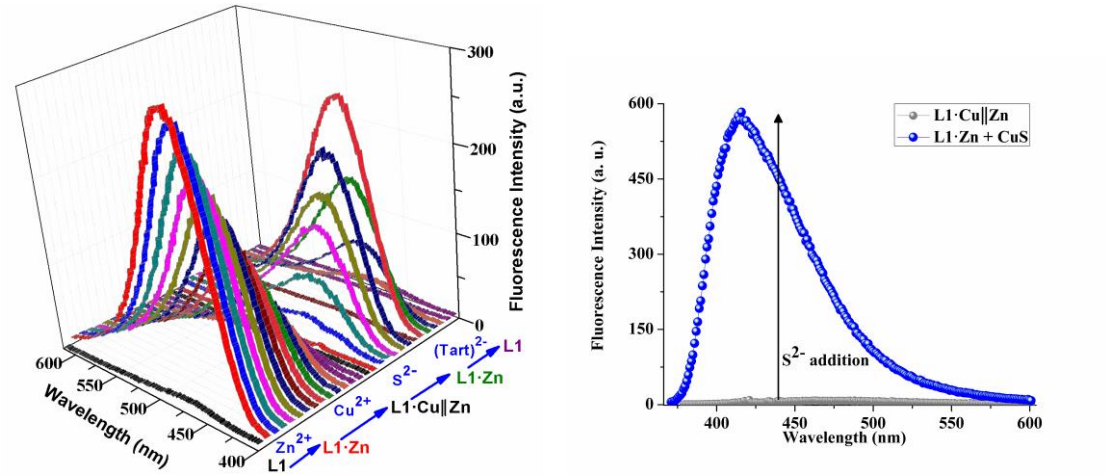

Figure S12. FACS flow cytometry for **L2** with Zn^{2+} and Cu^{2+} .Jurkat cells were cultured in the presence of 20 μM of Zn^{2+} and 20 μM of Cu^{2+} for 4 hours, then **L2** was incubated for 30 min. Dot plots show forward scatter (FSC-A) *vs*. side scatter (SSC-A) and histograms show fluorescence intensity at 450 nm. Gated cells were selected according to side (FSC-A) and complexity (SSC-A) and emission of fluorescence at 450 nm was analyzed on live cells (histograms). Dead cells were excluded during acquisition by using propidium iodide (PI).

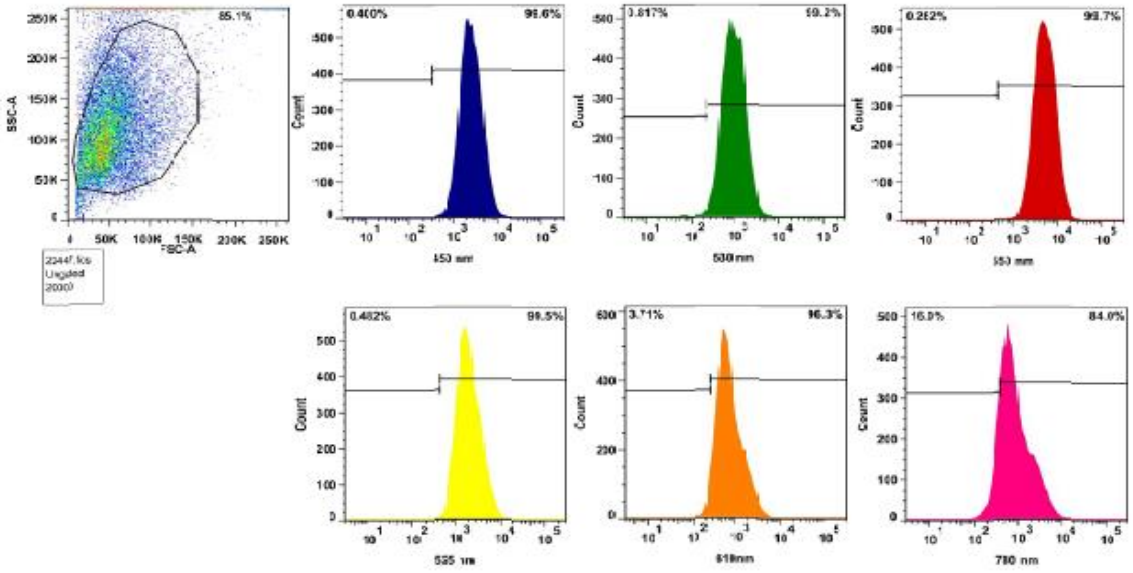

Figure S13. Computed (PBE0/6-31G(d)/PCM): a) mapped electrostatic potential for; b) difference in total electron density computed for the ground and first excited states; b) D_{CT} graphical representation; and c) centroids of charge ($C_+(r)/C_-(r)$, representing the excess electron density in the ground (green) and excited (red) state, for **L1** (left) and **L2** (right). Reference 28-29 from the Main text or references 3 and 4 from this file.

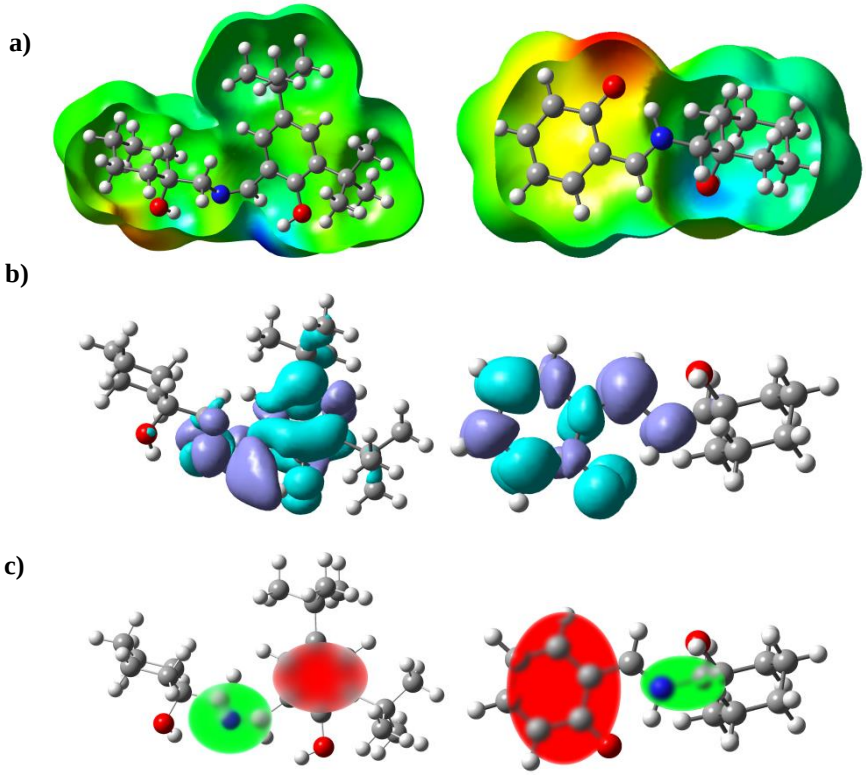

We studied the charge transfer excitation parameters by means of the recently proposed spatial extent index [28-29] For **L1** the obtained fraction of electron charge transferred upon de-excitation from the local excited (LE) state was q_{CT} = 0.51 at a D_{CT} = 2.75 Å spatial distance from the donor centroid to the acceptor centroid. Moreover, the dipole moment difference was estimated to be 6.68 D. Thus, Figure S8 shows the graphical representation of D_{CT}, and excess of electron density centroids ($C_+(r)/C_-(r)$) as defined in refs [28-29]. The *H* index defined as half of the sum of the centroid axis along the Donor – Acceptor direction is 1.18 Å, which resulted to be 1.58 Å lower than the CT excitation length, this means almost no overlap between donor and acceptor centroids, which makes the CT process highly efficient. However, in the case of **L2** being a more rigid ligand, the electronic communication obtained by means of this spatial extent index revealed a q_{CT} = 0.62 at a D_{CT} = 1.97 Å spatial distance from the donor to the acceptor centroid, representing a larger fraction of electron charge transferred, despite the smaller transition dipole moment of 5.01 D. The obtained spatial distance for **L2** is larger; hence, the difference between *H* index = 1.47 Å represents less overlap between donor and acceptor centroids, which makes the CT process highly efficient.

Table S1. (a) Molecular Orbital contribution; Oscillator strength (f); transition wavelength (nm) and energy (eV) values and NTO coefficient (*w*) for the free ligand **L2**, **L2•Zn** and **L2•Cu**. (b) NTO pairs for sensor **L1**.

(a)

Electronic transition	Properties	Hole	Electron	Assign
$S_0 \rightarrow S_1$	HOMO – LUMO; f = 0.174; 372 nm (3.33 eV) w = 0.94	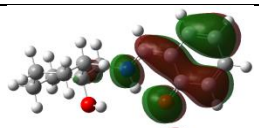	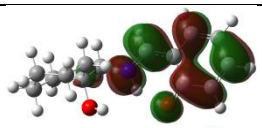	*Sal* π → *Sal* π*
$S_0 \rightarrow S_3$	HOMO-1 – LUMO+2 f = 0.091; 348 nm (3.56 eV) w = 0.82	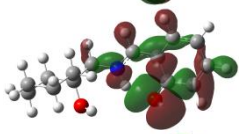	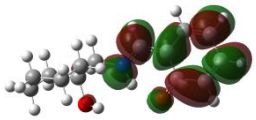	*Sal* π → *Sal* π*
$S_0 \rightarrow S_6$	HOMO-2 – LUMO+1; f = 0.369; 265 nm (4.17 eV) w = 0.78	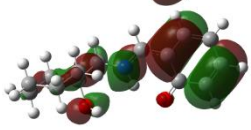	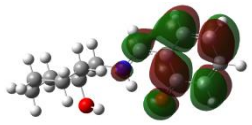	π → *Sal* π*
$S_0 \rightarrow S_2$	HOMO – LUMO+1; f = 0.183; 354 nm (3.50 eV) w = 0.86	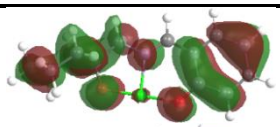	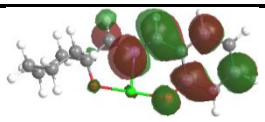	^{1}MLCT; $d_{x^2-y^2}$ π→*Sal*-π*
$S_0 \rightarrow S_5$	HOMO-1 –LUMO+2; f = 0.091; 366 nm (3.37 eV) w = 0.89	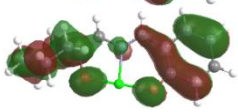	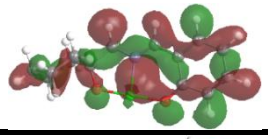	^{1}MLCT; π → *all*-π*
$S_0 \rightarrow S_1$	HOMO –LUMO; f = 0.078; 328 nm (3.78 eV) w = 0.81	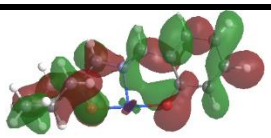	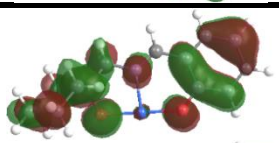	d_z^2 π → *all*-π*
$S_0 \rightarrow S_2$	HOMO-1 –LUMO+1; f = 0.142; 367 nm (3.37 eV) w = 0.92	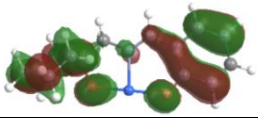	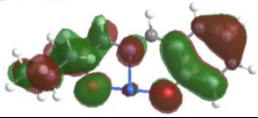	*all*-π → *all*-π*

(b)

$S_0 \rightarrow S_1$	HOMO – LUMO; f = 0.236; 328 nm (3.78 eV) w = 0.92	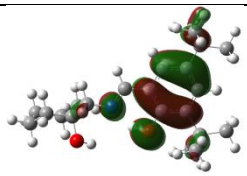	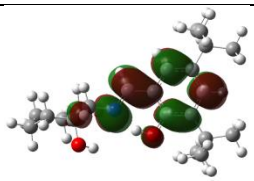	*Sal* π → *Sal* π*
$S_0 \rightarrow S_3$	HOMO-1 – LUMO+2 f = 0.063; 302 nm (4.10 eV) w = 0.87	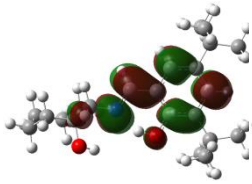	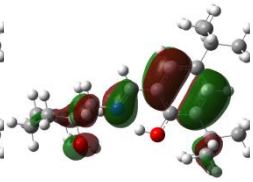	*Sal* π → *Sal* π*

1 S. Fery-Forgues, D. Lavabre, *J. Chem. Educ.*, 1999, **76**, 1260.

2 O. Domínguez, B. Rodríguez-Molina, M. Rodríguez, A. Ariza, N. Farfán, R. Santillan, *New J. Chem.*, 2011, **35**, 156.

3 M. J. Frisch, G. W. Trucks, H. B. Schlegel, G. E. Scuseria, M. A. Robb, J. R. Cheeseman, *et al.* Gaussian 03, Revision C.02, Wallingford CT, Gaussian, Inc., 2004.

4 C. Adamo, D. Jacquemin, *Chem. Soc. Rev.*, 2013, **42**, 845.